

Chapter 2

Surface Plasmon Resonance

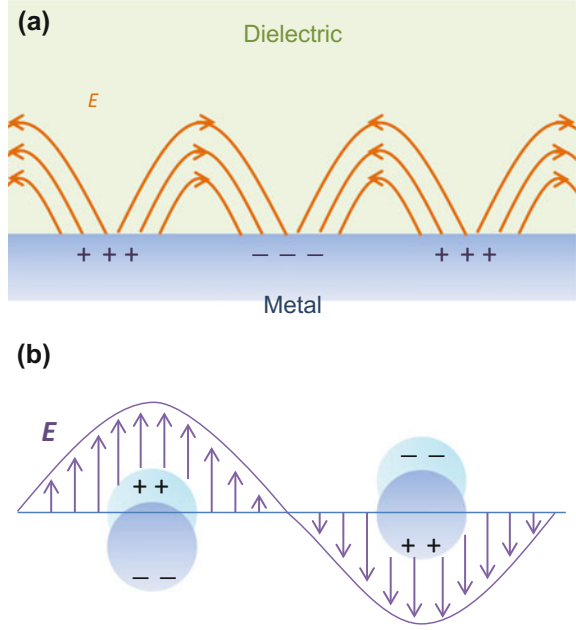
2.1 Introduction

Free electrons in metals behave like a gas of free charge carriers (also known as a plasma). The quanta corresponding to plasma oscillations are called plasmons. They exist in two forms: bulk plasmons in the volume of the material and surface plasmons which are bound at the metal-dielectric interface [1]. Surface plasmons originate from the interactions between free electrons and an incident electromagnetic (EM) wave. Hence, one picture describes a surface plasmon as a propagating electron density wave occurring at the metal/dielectric interface; Alternatively, it can also be viewed as a bound electromagnetic wave that propagates at an interface [2]. Such propagating wave is more specifically termed as a surface plasmon polariton (SPP) to differentiate it from the localized surface plasmon in small nanoparticles. One schematic of SPP is shown in Fig. 2.1a. For small metallic particles with sizes comparable to the penetration depth of an EM wave in a metal, the distinction between bulk plasmon and surface plasmon disappears. The EM field penetrates into the metallic particles and shifts the free electrons with respect to the metal ion lattice, which results in a restoring local field. The coherent interplay between the local field and the shift of electrons yield a resonance referred to as the localized surface plasmon resonance (LSPR) (Fig. 2.1b). Next, with the aid of simple models, we proceed to provide a mathematical description of a surface plasmon.

2.2 Surface Plasmon Polariton

The dispersion relation of SPP modes (i.e., frequency—wavevector relationship) is obtained by solving the Helmholtz equation:

Fig. 2.1 **a** Schematic of surface plasmon polaritons. **b** Schematic of localized surface plasmon resonance



$$\nabla^2 \mathbf{E} + k_0^2 \epsilon \mathbf{E} = 0, \quad (2.1)$$

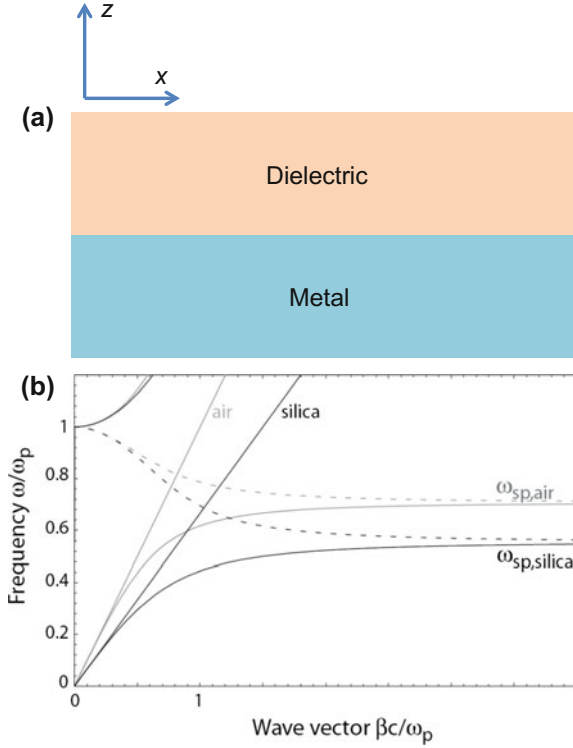
where \mathbf{E} the oscillating electric field $\mathbf{E}(\mathbf{r}, t) = \mathbf{E}(\mathbf{r})e^{-i\omega t}$ and $k_0 = \frac{\omega}{c}$ is the wavevector in vacuum. For the simplest geometry: a single, flat interface between a non-absorbing dielectric in one half space and a metal plate in the other half space (Fig. 2.2a), the dispersion relation can be easily solved by applying suitable boundary conditions:

$$k_{SPP} = k_0 \sqrt{\frac{\epsilon_m \epsilon_d}{\epsilon_m + \epsilon_d}}, \quad (2.2)$$

where ϵ_m and ϵ_d are the dielectric constant of the metal and the dielectric layer, respectively. In the free electron model of the electron gas with negligible damping, the dielectric constant of the metal is: $\epsilon_m = 1 - \frac{\omega_p^2}{\omega^2}$, where ω_p is the plasma frequency.

Figure 2.2b shows the dispersion relation of SPPs at the interface between a Drude metal and air (gray curves $\epsilon_d = 1$) and silica (black curves $\epsilon_d = 2.25$). The solid and broken curves are the real and imaginary parts of the wavevector, respectively. In the retarded regime when the frequencies approach zero, the SPP wavevectors approach the light wavevector k_0 ; whereas in the opposite non-retarded regime of large wavevectors, the SPP frequencies approach the surface plasmon frequencies:

Fig. 2.2 **a** Layout of a 1-D interface for SPP. **b** SPPs dispersion relation at the silver and dielectric interface. Adapted from reference [3]



$$\omega_{SP} = \frac{\omega_p}{\sqrt{1 + \epsilon_d}}. \quad (2.3)$$

Notice that there is no crossing between the light lines and the SPP curves, i.e., the wavevector of SPP mode is always larger than that of light at the same frequency. Hence, it is impossible to excite the SPP at an ideal planar interface directly with light. To couple light into the SPP, phase-matching methods have to be used. A grating or prism can be used for exciting the SPP with light. As shown in Fig. 2.2b, the light line in the silica glass intersects with the SPP at the metal/air interface at a certain point, where the phase-matching condition is satisfied.

At a real metal/dielectric interface, the SPP propagates but will gradually attenuate due to absorption losses in the metal. The propagation length can be obtained from the imaginary part of the complex SPP wavevector, $k_{SPP} = k'_{SPP} + ik''_{SPP}$. It can be expressed as [4]:

$$\delta_{SPP} = \frac{1}{2k''_{SPP}} = \frac{c}{\omega} \left(\frac{\epsilon_1 + \epsilon_d}{\epsilon_1 \epsilon_d} \right)^{\frac{3}{2}} \frac{\epsilon_1^2}{\epsilon_2}, \quad (2.4)$$

where $\epsilon_m = \epsilon_1 + i\epsilon_2$ is the dielectric constant of the metal. For example, silver which has the lowest loss in metals have a propagation length of 22 μm at 515 nm and reaches 500 μm at 1060 nm. Meanwhile, SPP also attenuates evanescently perpendicular to the metal interface and can be quantified using the skin depth:

$$L_{m(d)} = \frac{c}{\omega} \sqrt{\frac{\epsilon_m + \epsilon_d}{-\epsilon_{m(d)}^2}}. \quad (2.5)$$

The skin depth in dielectric layer is usually longer than that in the metal. For example, for silver, at 600 nm wavelength, the skin depth in the metal layer is 24 nm while in air, it is 390 nm [5].

2.3 Localized Surface Plasmon Resonance

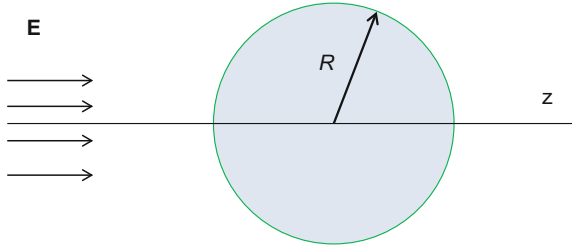
Localized surface plasmons are non-propagating free electron density waves that are coupled to the EM field. Consider the simplest structure: a metallic sphere with a diameter R surrounded by a uniform dielectric environment (dielectric constant: ϵ_d) and an EM field $\mathbf{E} = E_0 \mathbf{z}$ passes through it (Fig. 2.3). Using the Laplace equation for the potential $\nabla^2 \Phi = 0$ to obtain the field distribution in the vicinity of the metallic sphere, we have:

$$\Phi(r, \theta) = \sum_{l=0}^{\infty} \left[A_l r^l + B_l r^{-(l+1)} \right] P_l(\cos \theta). \quad (2.6)$$

As the potential is finite at $r = 0$ and $r \rightarrow \infty$, we have:

$$\Phi(r, \theta) = \sum_{l=0}^{\infty} A_l r^l P_l(\cos \theta) \quad (r \leq R) \quad (2.7)$$

Fig. 2.3 Schematic of a metal sphere in a uniform external field



$$\Phi(r, \theta) = \sum_{l=0}^{\infty} B_l r^l + C_l r^{-(l+1)} P_l(\cos \theta) \quad (r \geq R) \quad (2.8)$$

Applying the boundary conditions at $r = R$

$$-\frac{1}{R} \frac{\partial \Phi(r, \theta)}{\partial \theta} \Big|_{r \rightarrow R^-} = -\frac{1}{R} \frac{\partial \Phi(r, \theta)}{\partial \theta} \Big|_{r \rightarrow R^+} \quad (2.9)$$

$$-\varepsilon_m \varepsilon_0 \frac{\partial \Phi(r, \theta)}{\partial r} \Big|_{r \rightarrow R^-} = -\varepsilon_d \varepsilon_0 \frac{\partial \Phi(r, \theta)}{\partial r} \Big|_{r \rightarrow R^+} \quad (2.10)$$

and at $r \rightarrow \infty$,

$$\Phi|_{r \rightarrow \infty} = -E_0 r \cos \theta \quad (2.11)$$

The potential distribution can be obtained:

$$\Phi = -\frac{3\varepsilon_d}{\varepsilon_m + 2\varepsilon_d} E_0 r \cos \theta \quad (r \leq R) \quad (2.12)$$

$$\Phi = -E_0 r \cos \theta + \frac{\varepsilon_m - \varepsilon_d}{\varepsilon_m + 2\varepsilon_d} E_0 R^3 \frac{\cos \theta}{r^2} \quad (r \geq R) \quad (2.13)$$

The electric potential outside the sphere comprises of the applied electric field contribution and that from the field-induced dipole in the sphere:

$$\mathbf{p} = 4\pi\varepsilon_0\varepsilon_d \frac{\varepsilon_m - \varepsilon_d}{\varepsilon_m + 2\varepsilon_d} \mathbf{E} \quad (2.14)$$

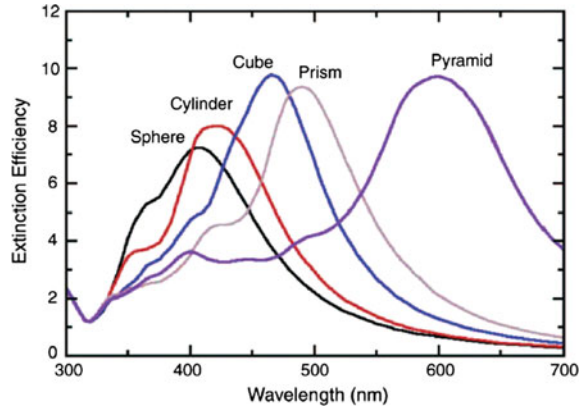
The dipole is at resonance when $\varepsilon_m + 2\varepsilon_d$ reaches a minimum, which is referred to as the LSPR. The resonance frequency is sensitive to the dielectric constant of the environment the metal nanoparticle located in and the metal's dielectric response to the EM wave.

In 1908, Professor Gustav Mie gave an exact analytical description of the optical behavior of sub-micrometer metallic nanoparticles [6]. For particles much smaller than incident wavelength, only the dipole oscillation contributes to the absorption and scattering, Mie's theory for nanosphere can be approximated into:

$$\gamma_{abs} = NV \frac{18\pi\varepsilon_d^{3/2}}{\lambda} \frac{\varepsilon_2}{(\varepsilon_1 + 2\varepsilon_d)^2 + \varepsilon_2^2}, \quad (2.15)$$

$$\gamma_{sca} = NV \frac{4\pi a^3 \varepsilon_d^{1/2}}{\lambda} \frac{(\varepsilon_1 - \varepsilon_d)^2 + \varepsilon_2^2}{(\varepsilon_1 + 2\varepsilon_d)^2 + \varepsilon_2^2} \quad (2.16)$$

Fig. 2.4 Extinction efficiency of silver nanoparticles with different shapes. Adapted from reference [9]



where N is the number of spheres per unit volume; V is the volume of each sphere; λ is the light wavelength; ε_1 and ε_2 are the real and imaginary part of the metal dielectric constant $\varepsilon_m = \varepsilon_1 + i\varepsilon_2$ [7]. When $\varepsilon_1 + 2\varepsilon_d = 0$, the absorption and scattering reaches a resonant maximum, corresponding to the LSPR of the metallic sphere. Professor Richard Gans extended Mie's theory to prolate and oblate ellipsoids by adding a depolarization factor [7, 8]. More complex systems require computational methods such as finite-difference time domain (FDTD), discrete-dipole approximation (DDA) etc., to obtain an approximate solution of the optical properties. Figure 2.4 displays the extinction efficiency (i.e., ratio of the cross section to the effective area) of silver nanoparticles having different shapes. The LSPR peak position is very sensitive to the shape of the nanostructures [9].

2.4 Summary

A succinct description of surface plasmons and their underlying theories has been presented. For more details, the interested reader is directed to many excellent books on plasmonics [2–4, 10, 11].

References

1. Brongersma ML, Kik PG. Surface plasmon nanophotonics. Dordrecht: Springer; 2007.
2. Schasfoort RBM, Tudos AJ. Handbook of surface plasmon resonance. Cambridge: RSC Pub.; 2008.
3. Maier SA. Plasmonics: fundamentals and applications. 1st ed. Berlin: Springer; 2007.
4. Raether H. Surface plasmons on smooth and rough surfaces and on gratings. Berlin: Springer; 1988.

5. Lakowicz JR. Radiative decay engineering 5: metal-enhanced fluorescence and plasmon emission. *Anal Biochem.* 2005;337(2):171–94.
6. Mie G. Beiträge zur Optik trüber Medien, speziell kolloidaler Metallösungen. *Ann Phys.* 1908;330(3):377–445.
7. Papavassiliou GC. Optical-properties of small inorganic and organic metal particles. *Prog Solid State Chem.* 1979;12(3–4):185–271.
8. Gans R. Über die Form ultramikroskopischer Goldteilchen. *Ann Phys.* 1912;342(5):881–900.
9. Haes AJ, Haynes CL, McFarland AD, Schatz GC, Van Duyne RR, Zou SL. Plasmonic materials for surface-enhanced sensing and spectroscopy. *MRS Bull.* 2005;30(5):368–75.
10. Enoch S, Bonod N. *Plasmonics: from basics to advanced topics*, vol. 167. Berlin: Springer; 2012.
11. Shahbazyan TV, Stockman MI. *Plasmonics: theory and applications*. 1st edn, vol 15. Berlin: Springer; 2013.

<http://www.springer.com/978-981-10-2019-3>

Plasmonic Organic Solar Cells

Charge Generation and Recombination

Wu, B.; Mathews, N.; Sum, T.-C.

2017, IX, 106 p. 77 illus., 73 illus. in color., Softcover

ISBN: 978-981-10-2019-3